

Novel lithium insertion material of $\text{LiCo}_{1/3}\text{Ni}_{1/3}\text{Mn}_{1/3}\text{O}_2$ for advanced lithium-ion batteries

Naoaki Yabuuchi, Tsutomu Ohzuku*

Electrochemistry and Inorganic Chemistry Laboratory, Department of Applied Chemistry, Graduate School of Engineering, Osaka City University (OCU), Sugimoto 3-3-138, Sumiyoshi, Osaka 558-8585, Japan

Abstract

A novel lithium insertion material of $\text{LiCo}_{1/3}\text{Ni}_{1/3}\text{Mn}_{1/3}\text{O}_2$ was reported for advanced lithium-ion batteries. $\text{LiCo}_{1/3}\text{Ni}_{1/3}\text{Mn}_{1/3}\text{O}_2$ ($R\bar{3}m$; $a = 2.862(2)$ Å and $c = 14.227(8)$ Å in hexagonal setting) shows about 200 mAh g^{-1} of rechargeable capacity with rate capability as high as 1.6 A g^{-1} between voltages of 2.5 and 4.6 V. Preliminary cycle tests of a $\text{Li}/\text{LiCo}_{1/3}\text{Ni}_{1/3}\text{Mn}_{1/3}\text{O}_2$ cell were also carried out for 30 cycles and shows that loss of rechargeable capacity was negligible. Thermal behavior of fully charged $\text{LiCo}_{1/3}\text{Ni}_{1/3}\text{Mn}_{1/3}\text{O}_2$ was examined by differential scanning calorimetry and shown that the exothermic reaction of $\square_{0.88}\text{Li}_{0.12}\text{Co}_{1/3}\text{Ni}_{1/3}\text{Mn}_{1/3}\text{O}_2$ with electrolyte is much milder than that of $\square\text{NiO}_2$ or $\square\text{CoO}_2$. From these results we have discussed whether or not this material can be used for advanced lithium-ion batteries.

© 2003 Elsevier Science B.V. All rights reserved.

Keywords: Lithium insertion material; Lithium-ion battery; Lithium cobalt nickel manganese oxides

1. Introduction

During the past 10 years, lithium-ion batteries with LiCoO_2 [1] and graphite [2] have been developed to a quite high level. Energy density based on weight or volume, however, will become saturated in the near future unless material innovations can be made. One of the strategies to advance lithium-ion batteries in terms of the energy density is to extend rechargeable capacity of the positive-electrode material to more than 200 mAh g^{-1} . Among candidate materials reported so far, such as LiNiO_2 [3], more generally $\text{LiCo}_x\text{Ni}_{1-x}\text{O}_2$ [4], or $\text{LiAl}_{1/4}\text{Ni}_{3/4}\text{O}_2$ [5], etc. no material can store and deliver electricity more than 200 mAh g^{-1} in a useful voltage range. After several trials from both theory and practice [6,7], a series of lithium nickel manganese oxides with or without cobalt has been proposed [6–9] for advanced lithium-ion batteries. In this paper we report on the cycle behavior and rate capability of lithium cells with $\text{LiCo}_{1/3}\text{Ni}_{1/3}\text{Mn}_{1/3}\text{O}_2$.

2. Experimental

$\text{LiCo}_{1/3}\text{Ni}_{1/3}\text{Mn}_{1/3}\text{O}_2$ was prepared from $\text{LiOH}\cdot\text{H}_2\text{O}$ and a triple hydroxide of cobalt, nickel, and manganese (MX-016, Co:Ni:Mn = 0.98:1.02:0.98, Tanaka Chemical Corp. Ltd.).

Starting materials were well mixed and pressed into pellets (23 mm diameter and ca. 5 mm thickness). The pellets were predried at 150 °C in air for 1 h and then heated at 1000 °C for 14 h in air. The reaction product was ground into powder using a mortar and pestle and stored in a desiccator over blue silica-gel before use. The samples were characterized by X-ray diffraction (XRD) using an X-ray diffractometer (XD-3A, Shimadzu Corp., Japan) with copper $\text{K}\alpha$ radiation. The system was equipped with a diffracted graphite monochromator.

In preparing the electrodes, polyvinylidene fluoride (PVdF) dissolved in *N*-methyl-2-pyrrolidone (NMP) solution was used as a binder. The black viscous slurry consisting of 88 wt.% $\text{LiCo}_{1/3}\text{Ni}_{1/3}\text{Mn}_{1/3}\text{O}_2$, 6 wt.% acetylene black, and 6 wt.% PVdF was cast on an aluminum foil (15 mm × 20 mm) with blade. Then, NMP was evaporated at 120 °C for 30 min, and finally the electrodes were dried under vacuum at 150 °C for 15 h. A lithium electrode was prepared by pressing a lithium metal onto a stainless steel sheet (15 mm × 20 mm). Two sheets of porous polypropylene membrane (Celgard 2500) were used as a separator. The electrolyte used was 1 M LiPF_6 dissolved in ethylene carbonate (EC)/dimethyl carbonate (DMC) (3/7 v/v) solution.

For differential scanning calorimetry (DSC), charged sample of $\text{LiCo}_{1/3}\text{Ni}_{1/3}\text{Mn}_{1/3}\text{O}_2$, LiNiO_2 , or LiCoO_2 was electrochemically prepared using a compressed pellet of the samples without adding any conductive or organic binder (forming pressure: 10^3 kg cm^{-2} ; 11.3 mm diameter

* Corresponding author.

E-mail address: ohzuku@chem.eng.osaka-cu.ac.jp (T. Ohzuku).

and ca. 0.6 mm thickness). The electrochemical oxidation of the pellets was performed galvanostatically at 0.3 mA cm^{-2} while monitoring the cell voltage. The samples (11–13 mg) containing electrolyte was sealed in an aluminum cell (5.5 mm diameter and ca. 1 mm thickness). Twelve milligrams of $\alpha\text{-Al}_2\text{O}_3$ in the aluminum cell was used as a reference. All procedures for handling and fabricating the electrochemical cells were performed in an argon-filled glove box.

The electrochemical cells and the data acquisition system used in this study are the same as described in a previous paper [10]. Other sets of experimental conditions are given in Section 3.

3. Results and discussion

Fig. 1 shows the XRD patterns of LiNiO_2 , $\text{LiCo}_{1/3}\text{Ni}_{1/3}\text{Mn}_{1/3}\text{O}_2$, and LiCoO_2 . The XRD pattern of $\text{LiCo}_{1/3}\text{Ni}_{1/3}\text{Mn}_{1/3}\text{O}_2$ is quite similar to that of LiCoO_2 [11] or LiNiO_2 [3]. The lattice parameters of $\text{LiCo}_{1/3}\text{Ni}_{1/3}\text{Mn}_{1/3}\text{O}_2$ for the nine identical samples reported here are calculated to be $a = 2.862(2) \text{ \AA}$ and $c = 14.227(8) \text{ \AA}$ in a hexagonal setting. The values are averages for nine samples. The parameters for each sample were obtained by a least squares method using 11 diffraction lines. Among LiNiO_2 , $\text{LiCo}_{1/3}\text{Ni}_{1/3}\text{Mn}_{1/3}\text{O}_2$, and LiCoO_2 in Fig. 1, LiCoO_2 has the smallest lattice constant and unit cell volume, i.e. $a = 2.819(2) \text{ \AA}$, $c = 14.069(4) \text{ \AA}$ and 96.8 \AA^3 , and LiNiO_2 has the largest unit cell volume of 102.3 \AA^3 . The unit cell volume

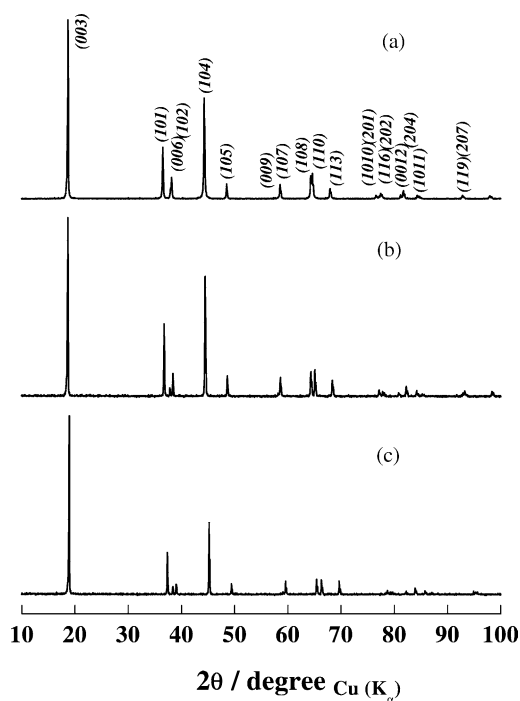


Fig. 1. X-ray diffraction patterns of (a) LiNiO_2 , (b) $\text{LiCo}_{1/3}\text{Ni}_{1/3}\text{Mn}_{1/3}\text{O}_2$, and (c) LiCoO_2 .

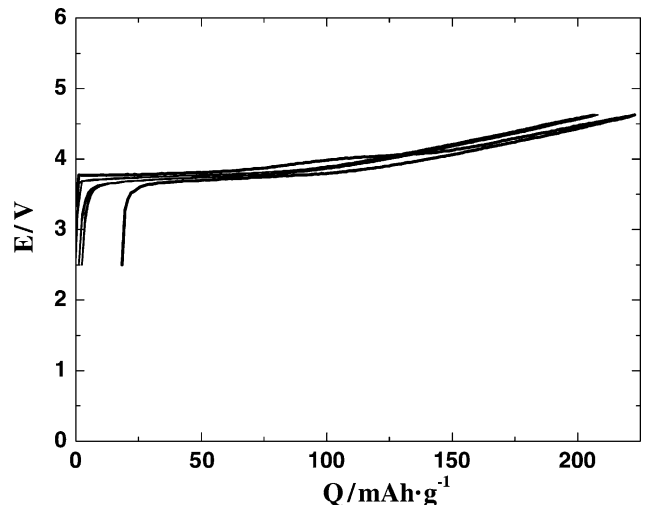


Fig. 2. Charge and discharge curves of a $\text{Li/LiCo}_{1/3}\text{Ni}_{1/3}\text{Mn}_{1/3}\text{O}_2$ cell operated at 0.17 mA cm^{-2} in voltages of 2.5–4.6 V at 30°C . The sample weight loaded was 0.0341 g . The first charge and discharge curves are deviated from the subsequent charge and discharge curves which converge to a steady curve.

of $\text{LiCo}_{1/3}\text{Ni}_{1/3}\text{Mn}_{1/3}\text{O}_2$ is 100.6 \AA^3 , which is midway between LiCoO_2 and LiNiO_2 .

Fig. 2 shows the charge and discharge curves of a $\text{Li/LiCo}_{1/3}\text{Ni}_{1/3}\text{Mn}_{1/3}\text{O}_2$ cell operated at 0.17 mA cm^{-2} between 2.5 and 4.6 V at 30°C . As seen in Fig. 2, $\text{LiCo}_{1/3}\text{Ni}_{1/3}\text{Mn}_{1/3}\text{O}_2$ shows 200 mAh g^{-1} of rechargeable capacity. On charging at 0.17 mA cm^{-2} , the voltage rapidly increased to about 3.7 V and then stayed along an almost horizontal line at 3.75 V, that is ca. 0.2 V lower operating voltage than that of LiCoO_2 , until the charge capacity reaches 90–95 mAh g^{-1} . The slope in the E versus Q curves increased at 90–95 mAh g^{-1} and voltage curves linearly increased until voltage reaches 4.6 V. The irreversible capacity usually observed in the first cycle was about 20 mAh g^{-1} .

In order to examine whether or not a kinetic limitation of lithium-ion transfer in the solid state was important in the $\text{LiCo}_{1/3}\text{Ni}_{1/3}\text{Mn}_{1/3}\text{O}_2$ electrode, the rate-capability tests were carried out. The results are shown in Fig. 3. To measure the rate capability the cell was charged at $0.17\text{--}14.7 \text{ mA cm}^{-2}$ until the voltage reached 4.6 V and then discharged at $0.17\text{--}14.7 \text{ mA cm}^{-2}$ corresponding to $18.3\text{--}1600 \text{ mA g}^{-1}$ based on $\text{LiCo}_{1/3}\text{Ni}_{1/3}\text{Mn}_{1/3}\text{O}_2$ weight. The discharge capacity observed is 200 mAh g^{-1} at 0.17 mA cm^{-2} or 18.3 mA g^{-1} . When the cell is discharged at 14.7 mA cm^{-2} or 1600 mA g^{-1} based on $\text{LiCo}_{1/3}\text{Ni}_{1/3}\text{Mn}_{1/3}\text{O}_2$ weight, 73% capacity is observed. In other words, if we define C-rate with respect to the 200 mAh g^{-1} observed at the low rate discharge of 18.3 mA g^{-1} , 8C-rate (1600 mA g^{-1}) discharge are possible for this sample.

Change in the charge and discharge capacities is shown in Fig. 4 as a function of cycle number for a cell operated at 0.17 mA cm^{-2} between 2.5 and 4.6 V. We selected 4.6 V, because this voltage is a critical upper limit for LiCoO_2 [11],

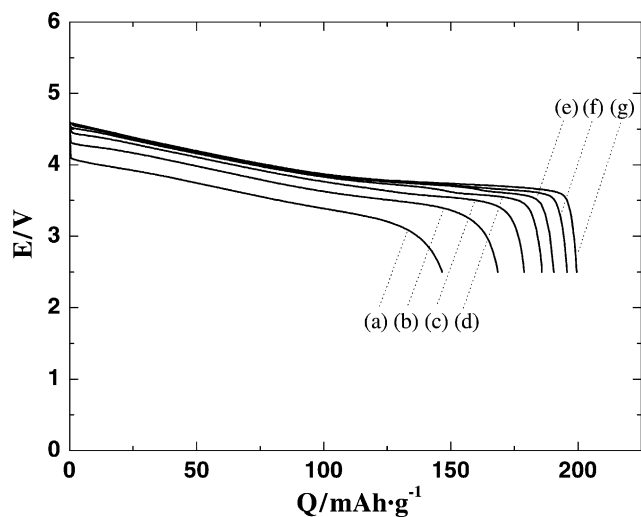


Fig. 3. Rate-capability tests on a $\text{Li}/\text{LiCo}_{1/3}\text{Ni}_{1/3}\text{Mn}_{1/3}\text{O}_2$ cell. The cell was charged at 0.17 mA cm^{-2} up to 4.6 V and then discharged to 2.5 V at (a) 14.7 mA cm^{-2} (1600 mA g^{-1} based on $\text{LiCo}_{1/3}\text{Ni}_{1/3}\text{Mn}_{1/3}\text{O}_2$ sample weight), (b) 7.3 (800), (c) 3.7 (400), (d) 1.8 (200), (e) 0.92 (100), (f) 0.46 (50.0), or (g) 0.17 (18.3). The sample weight loaded was 0.0272 g. The electrode thickness was 90 μm .

LiNiO_2 [3] or $\text{Li}[\text{Li}_x\text{Mn}_{2-x}]\text{O}_4$. As was reported previously [3], when a Li/LiNiO_2 cell was operated below 4.2 V, it cycles without any noticeable loss of rechargeable capacity. However, it deteriorates rapidly at voltages above 4.2 V due mainly to the formation of nickel dioxide. For the Li/LiCoO_2 cell, LiCoO_2 can be cycled over the composition range of $0 < x < 0.5$ in $\text{Li}_{1-x}\text{CoO}_2$ with a rechargeable capacity of 135–150 mAh g^{-1} . The upper limit of charge-end voltage is about 4.3 V for many reasons, such as cycle life, safety, gassing, and so forth. As can clearly be seen in Figs. 2 and 4, $\text{LiCo}_{1/3}\text{Ni}_{1/3}\text{Mn}_{1/3}\text{O}_2$ showed a rechargeable capacity of more than 200 mAh g^{-1} with excellent capacity retention. The charge and discharge coulombic efficiencies are

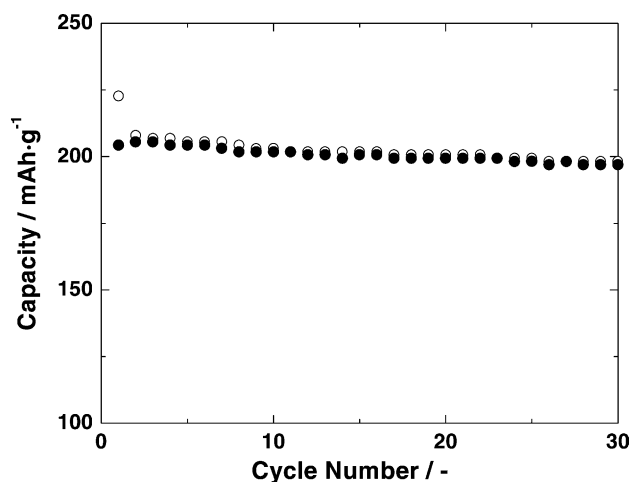


Fig. 4. Charge and discharge capacities as a function of cycle number for a cell operated at 0.17 mA cm^{-2} in voltages of 2.5–4.6 V at 30 °C. Open and closed circles indicate charge and discharge capacities, respectively.

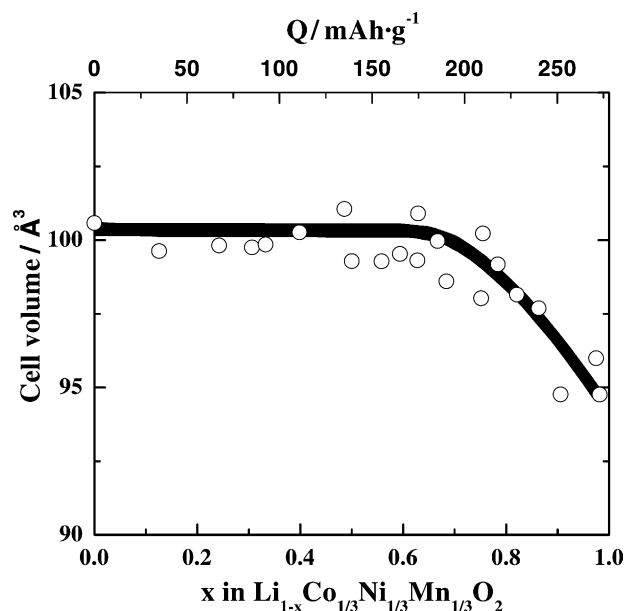


Fig. 5. Change in the unit cell volume as a function of x in $\text{Li}_{1-x}\text{Co}_{1/3}\text{Ni}_{1/3}\text{Mn}_{1/3}\text{O}_2$. Zero-volume change can be seen in $x = 0$ to 0.67.

approximately 99% in this case. Constant current charge followed by constant voltage charge (so-called CCCV) at 4.3–4.6 V is possible, although a better selection of electrolyte must be done to improve coulombic efficiency.

Fig. 5 shows the change in unit cell volume determined by ex situ XRD. For $0 \leq x \leq 0.67$ in $\text{Li}_{1-x}\text{Co}_{1/3}\text{Ni}_{1/3}\text{Mn}_{1/3}\text{O}_2$, the c -axis dimension elongated from 14.23 to 14.50 Å while the a -axis shortened from 2.86 to 2.82 Å (not shown). Consequently, the unit cell volume remains almost constant, i.e. zero-volume change until $x = 0.67$ in $\text{Li}_{1-x}\text{Co}_{1/3}\text{Ni}_{1/3}\text{Mn}_{1/3}\text{O}_2$. This is similar to the zero-volume change for $\text{LiCo}_{1/2}\text{Ni}_{1/2}\text{O}_2$ [12]. In the case of LiCoO_2 [11], the unit cell volume expands from 97 Å³ to a maximum value of 100 Å³ on charge, so that the unit cell volume of the charged state of LiCoO_2 is almost the same as that of $\text{LiCo}_{1/3}\text{Ni}_{1/3}\text{Mn}_{1/3}\text{O}_2$. Therefore, a lithium-ion cell with $\text{LiCo}_{1/3}\text{Ni}_{1/3}\text{Mn}_{1/3}\text{O}_2$ is expected to be equivalent to or superior to that with LiCoO_2 in terms of both gravimetric and volumetric energy densities.

The thermal behavior in the charged states of lithium insertion materials with electrolyte solution is key to considering suitability the positive electrodes for lithium-ion batteries. Fig. 6 shows the results on the DSC measurements for $\square_{0.88}\text{Li}_{0.12}\text{Co}_{1/3}\text{Ni}_{1/3}\text{Mn}_{1/3}\text{O}_2$, $\square_{0.88}\text{Li}_{0.12}\text{NiO}_2$ and $\square_{0.89}\text{Li}_{0.11}\text{CoO}_2$. The DSC samples were prepared electrochemically. After a constant-current charge at 0.3 mA cm^{-2} up to 5.0 V the electrode was taken out of the cell, and excess electrolyte (1 M LiPF_6 EC/DMC = 3/7) was wiped off with filter paper. A piece of the crushed pellet was mechanically sealed in an aluminum cell. The weight of the sample in the aluminum cells was calculated by measuring the cell weight with and without the sample. DSC signals were measured at a heating and cooling rate of $5 \text{ }^\circ\text{C min}^{-1}$.

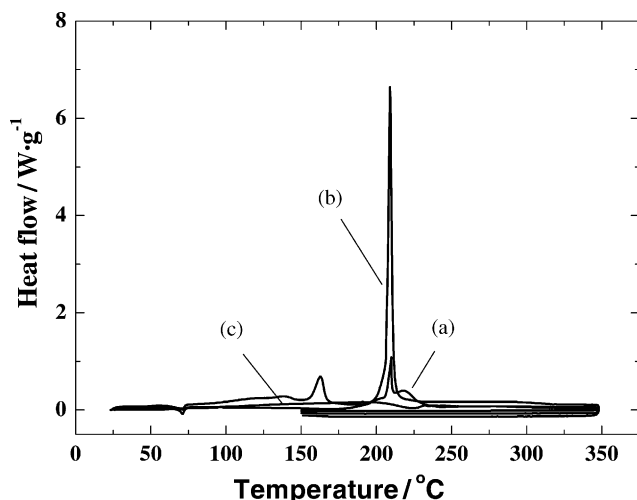


Fig. 6. DSC curves for (a) $\square_{0.88}\text{Li}_{0.12}\text{NiO}_2$, (b) $\square_{0.89}\text{Li}_{0.11}\text{CoO}_2$, and (c) $\square_{0.88}\text{Li}_{0.12}\text{Co}_{1/3}\text{Ni}_{1/3}\text{Mn}_{1/3}\text{O}_2$ containing electrolyte of 1 M LiPF_6 EC/DMC (3/7 v/v). The samples were prepared electrochemically using compressed pellets. Heating and cooling rates were 5°C min^{-1} .

The degree of oxidation x in $\text{Li}_{1-x}\text{Co}_{1/3}\text{Ni}_{1/3}\text{Mn}_{1/3}\text{O}_2$, $\text{Li}_{1-x}\text{NiO}_2$ or $\text{Li}_{1-x}\text{CoO}_2$ was calculated from the charge capacity and the theoretical capacity based on a one-electron transfer per $\text{LiCo}_{1/3}\text{Ni}_{1/3}\text{Mn}_{1/3}\text{O}_2$ (278 mAh g^{-1}), LiNiO_2 (275 mAh g^{-1}) or LiCoO_2 (274 mAh g^{-1}). As seen in Fig. 6, two exothermic spikes were observed at ca. 160 and 210 $^\circ\text{C}$ for charged LiCoO_2 and a spike at ca. 210 $^\circ\text{C}$ for the charged LiNiO_2 . Although some exothermic and endothermic reactions are involved in DSC signals on $\text{LiCo}_{1/3}\text{Ni}_{1/3}\text{Mn}_{1/3}\text{O}_2$, the thermal behavior of $\text{LiCo}_{1/3}\text{Ni}_{1/3}\text{Mn}_{1/3}\text{O}_2$ is milder than that of LiCoO_2 or LiNiO_2 .

As was described above, $\text{LiCo}_{1/3}\text{Ni}_{1/3}\text{Mn}_{1/3}\text{O}_2$ is equivalent to or better than LiCoO_2 , LiNiO_2 , or $\text{Li}[\text{Li}_x\text{Mn}_{2-x}\text{O}_4]$

for lithium-ion batteries. We believe that $\text{LiCo}_{1/3}\text{Ni}_{1/3}\text{Mn}_{1/3}\text{O}_2$ is a possible alternative to LiCoO_2 for advanced lithium-ion batteries.

Acknowledgements

One of us (T.O.) wishes to thank Mr. Hiroyuki Ito of Tanaka Chemical Corp., for his help on the preparation of nickel manganese hydroxide. The present work was partially supported by a grant-in-aid from the Osaka City University Science Foundation.

References

- [1] K. Mizushima, P.C. Jones, P.J. Wiseman, J.B. Goodenough, *Mater. Res. Bull.* 15 (1980) 783.
- [2] T. Ohzuku, Y. Iwakoshi, K. Sawai, *J. Electrochem. Soc.* 140 (1993) 2490.
- [3] T. Ohzuku, A. Ueda, M. Nagayama, *J. Electrochem. Soc.* 140 (1993) 1862.
- [4] T. Ohzuku, A. Ueda, M. Nagayama, Y. Iwakoshi, H. Komori, *Electrochim. Acta* 38 (1993) 1159.
- [5] T. Ohzuku, A. Ueda, M. Kouguchi, *J. Electrochem. Soc.* 142 (1995) 4033.
- [6] Y. Makimura, T. Ohzuku, in: *Proceedings of the 41st Battery Symposium on 2D20 and 2D21*, Nagoya, Japan, 2000.
- [7] Y. Koyama, I. Tanaka, H. Adachi, Y. Makimura, N. Yabuuchi, T. Ohzuku, in: *Proceedings of the 42nd Battery Symposium on 2I18 and 2I19*, Yokohama, Japan, 2001.
- [8] T. Ohzuku, Y. Makimura, *Chem. Lett.* (2001) 642.
- [9] Z. Lu, D.D. MacNeil, J.R. Dahn, *Electrochem. Solid-State Lett.* 4 (2001) A200.
- [10] T. Ohzuku, M. Kitagawa, T. Hirai, *J. Electrochem. Soc.* 136 (1989) 3169.
- [11] T. Ohzuku, A. Ueda, *J. Electrochem. Soc.* 141 (1994) 2972.
- [12] A. Ueda, T. Ohzuku, *J. Electrochem. Soc.* 141 (1994) 2010.